Single-phase ambient and cryogenic temperature heat transfer coefficients in microchannels*

S Baek and P E Bradley
Material Measurement Laboratory, National Institute of Standards and Technology, Boulder, CO 80305, USA

E-mail: sbaek@nist.gov, pbradley@nist.gov

Abstract. Micro-scaling cryogenic refrigerators, in particular the Joule-Thomson (JT) variety require very good information about heat transfer characteristics of the refrigerants flowing in the microchannels for optimal design and performance. The extremely low Reynolds flow is present in a micro JT cryocooler, the heat transfer characteristics at these conditions require investigation. There are numerous studies regarding heat transfer coefficient measurements of liquid flow in microchannels at/near ambient temperature and high Reynolds flow (Re>2000), that agree well with the conventional correlations. However, results from previous studies of gaseous flow in microchannels at low Reynolds flow (Re<1000) disagree with conventional theory. Moreover, the studies performed at cryogenic temperatures are quite limited in number. In this paper, the single-phase heat transfer coefficients and friction factors for nitrogen are measured at ambient and cryogenic temperatures. The hydraulic diameters for this study are 60, 110 and 180 μm for circular microchannels. The Reynolds numbers varied from a very low value of 10 to 3000. The measured friction factors are comparable to those in macro-scale tubes. The experimental results of the heat transfer indicate that Nusselt numbers derived from measurements are significantly affected by axial conduction at low Reynolds flow (Re<500). The Nusselt numbers at high Reynolds flow (Re>1000) follow conventional theory. The detailed experiment, procedure, and measured results are presented in this paper and discussed regarding deviation from ideal theory at low Reynolds flow.

1. Introduction

Lightweight and compact microcoolers are needed for advanced, hand-held infrared systems. To enable the use of sensors, temperatures around 150 K and refrigeration powers of 0.5 W are required for the new high performance infra-red sensors. Moreover, it is important to shrink the size of the cryocooler and reduce the mass to fabricate compact hand-held packages. For the development of small cryocoolers, previous researchers tried to fabricate Joule Thomson (JT) cryocoolers with microchannels.[1] The development of small JT cryocoolers inevitably requires the microchannel heat exchangers, which rises necessitates heat transfer characteristic information of fluids operating in the microchannels.

Previous microscale JT cryocoolers used either compressed cylinders of gas or relatively large compressors to feed the micro-cold head. The inlet pressures were usually greater than 8 MPa and pressure ratios were usually greater than 80:1. The flow rate was high enough to maintain the turbulent flow regime. The heat transfer characteristics of turbulent flow in the microchannels have been studied by other researchers [2, 3] and indicated that the Dittues Boelter and the Gnielinski correlations can be

* Contribution of NIST, not subject to copyright in the United States.

applied to the microchannels. Despite a very large number of published data, considerable discrepancies between the results still exist in laminar flow.

The microcryocooler for hand-held applications require micro-compressors, where high pressure ratios are not feasible. The previous work of University of Colorado, Boulder & National Institute of Standards and Technology [4, 5] focused on development of a mixed refrigerant JT cryocooler which operates at low pressure ratios, as low as 4:1. Lewis et al.[6] has showed that flow and temperature pulsations are present due to the two-phase flow of the mixed refrigerant in the microscale geometries. The pulsations resulted in a significant reduction of refrigeration power compared with the bulk thermodynamic value. For successful microcryocooler development, Radebaugh [7] introduced a cascade vapor compression cycle employing five refrigerants for a temperature of 150 K. Figure 1 shows a schematic of the five stage cascade cooler. In the design of the cascade compression cycles, isothermal and recuperative heat exchangers are also introduced to enhance performance of the cooler. The flow rate in each compression cycle is much lower than previous research due to the small temperature span of each stage. The flow regime in this case is laminar, where the Reynolds numbers are significantly less than 2000. Heat transfer characteristics of single-phase and two-phase fluids are required for recuperative and isothermal heat exchangers in low Reynolds regime, respectively.

In this study, the heat transfer characteristics of single-phase pure fluid is investigated for design of the heat exchangers for cascade vapor compression cycles. Previous research regarding single-phase heat transfer in laminar flow regime [8-10] reveals that Nusselt numbers are dependent on the Reynolds number. However, the results are not consistent with each other's experimental data. The measured Nusselt number varies in two order of magnitude. To provide useful design parameters, heat transfer coefficients of nitrogen fluid are measured in three different microchannels. In addition, gas and liquid flow are tested in the microchannel to observe the effects of property. These data will support two-phase heat transfer coefficients measurement in the microchannel for the further research. Moreover, the research on the nitrogen will support the heat transfer characteristics of refrigerants in the cascade cooler due to similar thermophyscial properties. Detailed experiment, procedure, and measured results are presented in this paper.

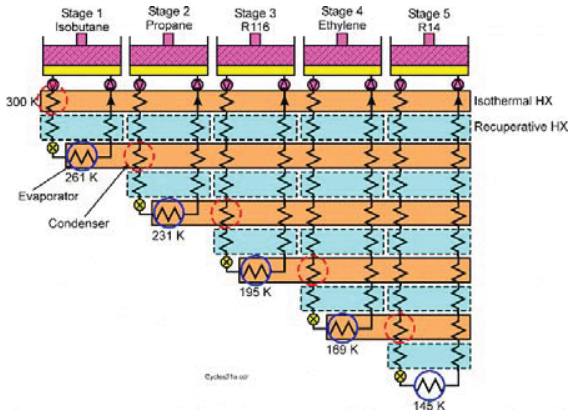

Figure 1. Schematic of a five-stage cascade cooler for 145 K showing isothermal and recuperative heat exchangers.[7]

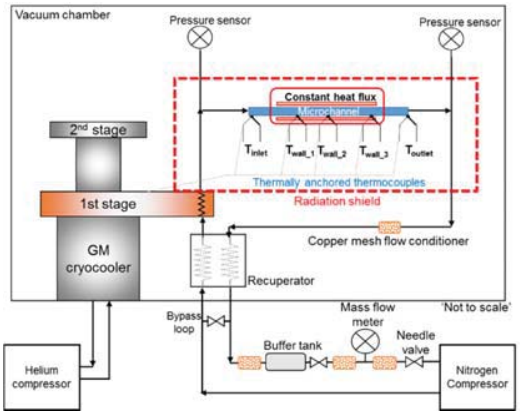

Figure 2. Experimental setup

2. Experimental method

The heat transfer coefficient under a constant heat flux condition is measured when forced convection of nitrogen flowing through microchannels. The wall temperatures, the pressure before and after the microchannel are measured to estimate the heat transfer coefficient inside the microchannel. Figure 2 displays the schematic of the experimental setup for measurement of the heat transfer coefficient of the fluid in a microchannel. A closed-loop setup including compressor, the microchannel test section, the

GM-cryocooler, and vacuum chamber is utilized for the experiment. The air-cooled oil-less compressor is located outside the vacuum chamber. In operation, compressed nitrogen from the compressor passes through the recuperator, along the 1st stage of the GM-cryocooler, and after passing through the microchannel, returns through the recuperator returning to the compressor. The recuperator is a custom counterflow heat exchanger fabricated with copper tubes that precools the inflow while preheating return flow to ambient temperature.

The test section is comprised of the microchannel, a wound heating wire, and several thermocouples.Table 1 gives length, hydraulic diameter (D_h), and outside diameter (D_{out}) of the microchannels. Figure 3 shows a close-up schematic of the test section. The microchannels are stainless steel 304. Five E-type thermocouples are soldered to the tinned microchannel wall prior to winding the heating wire. Three thermocouples are soldered at the 25%, 50% and 100% position along the heated length to measure the wall temperature of the microchannel. The remaining two thermocouples are soldered at the inlet wall and at the outlet wall of the microchannel to measure the inlet and the outlet temperature of the fluid. Because the thermocouple tip is larger than the inner diameter of the tube, thermocouples can't be installed inside the microchannel. The inlet and the outlet wall temperatures are assumed as the temperature of the fluid at those positions. The surface of the microchannel is cleaned with acetone after soldering the thermocouples. Prior to winding the heater, thermal grease is applied to the surface of the microchannel to improve the thermal contact between the heater and the microchannel. The heater wire diameter is 120 μm. A conductive epoxy is applied to complete the assembly. The microchannel is then soldered to metal gasket fittings that connect with copper tubes (6.35 mm OD) in the closed loop. The wound heating wire is electrically insulated so there are no electrical shunts with the thermocouples. The roughness of the microchannel is not measured in this study.

The test section is maintained in vacuum to a level of 10^{-4} torr or better to eliminate surrounding molecular conduction and convection effects. Further the microchannel assembly is surrounded by a thermal radiation shield heat sinked to the 1st stage of the GM-cryocooler. The mass flow meter is installed in the return stream to measure the flow rate of the circulating fluid. The flow rate in the closed loop is adjusted by a valve at the bypass loop near the compressor. Two pressure transducers are located at the entrance and the exit of the microchannel to measure the pressure drop across the microchannel. The heating power to the microchannel is also measured from the voltage drop and current across the heating wire. Electrical heating elements are attached to the 1st stage of the GM cryocooler to control the temperature of the nitrogen fluid to the microchannel. For the cryogenic experiment, GM-cryocooler is turned on to lower the temperature of the setup, and the current is applied to the heating elements with PID controlled power supplies to stabilize to the desired temperature for the setup. The measured temperature, pressure, flowrate, and power input to the microchannel are collected by data acquisition devices to a personal computer. The data are gathered every seconds and time-averaged for a minute. The uncertainty of the measured data is determined with the eqn. (1), where B is the total bias error and S is the standard deviation of the data.[11] The $t_{95\%}$ is 2.000 in this case.

$$U = \sqrt{B^2 + \left(t_{95\%} \frac{S}{\sqrt{N}} \right)} \tag{1}$$

Table 2 shows the error of the measurement and the total uncertainty of heat transfer coefficients (h). The uncertainty of Nusselt number is around 7 %.

Table 1 Specifications of microchannels used in the measurement

Microchannel	inside diameter $D_i=D_h$ (μm)	Outside diameter D_{out} (μm)	D_{in}/D_{out}	Total length (mm)	Heating length (mm)
D_h=180 μm	180±1	380	0.47	90	30
D_h=110 μm	110±1	310	0.35	80	30
D_h=65 μm	65±1	160	0.4	40	15

Table 2 Uncertainty analysis

Measurement	Range	Error
Temperature	77 K ~ 300 K	±0.1 K
Pressure	0 MPa ~ 1 MPa	±0.5%
Mass flow rate	0 sccm ~ 500 sccm	±0.5%
Total uncertainty of *Nu*		~7 %

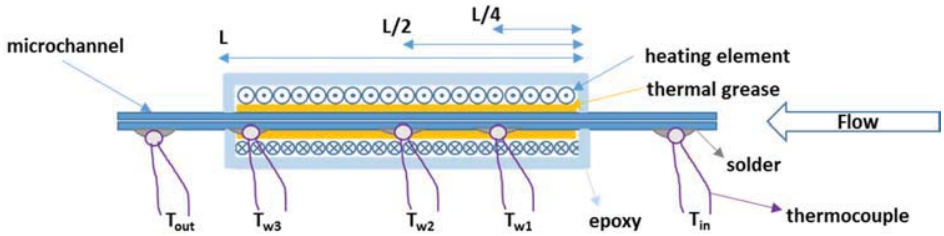

Figure 3 Schematic of the microchannel test section

The heat transfer coefficient of the fluid in the microchannel is estimated by classical method, so described accordingly by Yang *et al*[12], Morini *et al*[13], and Maranzana *et al.*[14] The heat transfer rate *q*, is measured from the DC power input deducted by the corresponding calibrated heat loss, which is equal to the increased enthalpy of nitrogen flow. Usually, it is assumed that the heat is added uniformly on the tube surface. Therefore, the local fluid temperature,$T_{f,x}$, at the position *x* from the heating entrance can be estimated by the assumption of linear temperature profile inside the channel:

$$q\frac{x}{L_h} = \dot{m}c_p(T_{f,x} - T_{in}) \tag{2}$$

where $\dot{m}$ is the mass flow rate, L_h is the channel heating length and T_{in} is the inlet temperature. From Newton's Law of cooling, the local heat transfer coefficient h_x can derived as eqn. (3),

$$h_x = \frac{q}{A(T_{w,x} - T_{f,x})} \tag{3}$$

where *A* is the heat transfer area, $A = \pi D_i L_h$, and D_i is the tube inside diameter. The circular channels are used, therefore D_i is identical to hydraulic diameter (D_h). The term $T_{w,x}$ is the local tube surface temperature that can be measured from the thermocouples. For the heat transfer coefficient calculation, T_{w2} from experiment is used and the inner wall temperature is estimated. The $T_{f,x}$ is calculated from the inlet and outlet temperatures as eqn. (4).

$$T_{f,50\%} = \frac{T_{in} + T_{out}}{2} \tag{4}$$

The Reynolds number is defined as follows:

$$\mathrm{Re}_x = \frac{GD_h}{\overline{\mu}} \tag{5}$$

where G is the flow mass flux defined as $G = \dot{m}/A_c$, A_c is the cross-sectional area of flow in the tube, and the viscosity ($\bar{\mu}$) of fluid is the averaged value from the inlet and the outlet. The viscosity can be calculated with the equation of state [15] obtained from REFPROP. The Nusselt number is defined as eqn. (6)

$$Nu_x = \frac{h_x D_h}{\bar{k}_f} \tag{6}$$

where the $\bar{k}_f$ is the thermal conductivity of the fluid, and it is averaged from the inlet and the outlet of the microchannel.

3. Results and Discussion

Figure 4 displays the measured friction factor from the experiment for three different microchannels. The friction factors are measured in adiabatic conditions. The friction factors are derived from the Fanning's equation.[16] The measured friction factors show an almost identical trend when the Reynolds numbers are below 2000. The measured values follow well with the laminar flow theory of f=16/Re. For the turbulent flow regime (Re>2000), the Blasius equation is compared to the The comparison shows that the measurements also show good agreement with the theory of f=16/Re within laminar regime. The maximum difference is 10% from theory. It can be inferred that friction factors of microchannels can be estimated similarly with those of macrochannels.

Figure 5 shows the estimated Nusselt number (eqn. (6)) from the measurements along the various Reynolds number. For the measurements of gaseous nitrogen in the microchannel, the inlet temperature to the microchannel is set at 296 K and the outlet temperature is maintained around 360 K. The dependency of Nusselt numbers on the Reynolds numbers are observed from the measurement as previous researchers observed. When the Reynolds numbers are around 1500, the Nusselt numbers show similar values to that of theory, 4.36. However, the Nusselt numbers decrease rapidly when the Reynolds numbers are below 1000. Moreover, the Nusselt numbers from D_h=180 μm microchannel show higher value than those from D_h=110 μm and 65 μm. The Nusselt number from D_h=110 μm show the minimum Nusselt numbers. The deviation between experimental results are due to the different wall thickness of miicrochannels.

The Nusselt numbers of liquid nitrogen flow through the microchannels are also indicated in Figure 5. The inlet temperatures are maintained at T_{in}=67 K, and the outlet temperatures are maintained around 87 K. The Nusselt numbers show very similar values to the theory (Nu=4.36) when the Reynolds numbers are from 100 to 2000. These results show completely different trend than the gas experiments. When the Reynolds numbers are below 100, the Nusselt numbers start to decrease. However, the amount of degradation is not comparable to those from the gas experiment. The trend of the Nusselt numbers for three different microchannels show similar declination trends at low Reynolds values below 50 for the liquid experiment.

Estimation of Nusselt number for two different phases for the identical fluid has not been reported for the microchannel. It is difficult to explain the different trend of Nussselt number by basic heat transfer theories. The different trend of Nusselt numbers for two different phases indicate that the measurement is affected by the thermophysical property of the fluid and the channel. Guo and Li[17] pointed out some scaling effects can influence the thermal behavior of gas flows through microchannels, in particular 1) gas rarefaction, 2) flow compressibility, 3) viscous dissipation, 4) axial conduction along the walls, and 5) axial conduction along the fluid. Each effect can be explained by non-dimensional numbers. The rarefaction effects can be related to the Knudsen number (Kn) defined as $Kn = \xi/d$. The term ξ is mean free path of fluid, and d is the characteristic length of the channel. In general, rarefaction effects can be considered negligible when Kn<0.001. Flow compressibility effects can be checked with the mean Mach Number (Ma). When Ma<0.3, compressibility effects can be ignored. The viscous dissipation effect can be checked by using the Brinkman number (Br) which is a measure of the importance of the viscous

Table 3 Typical range of non-dimensional parameters related to scaling effects for microchannels with nitrogen (Re=1~3000)

Microchannel	Phase	Kn (<0.001)	Ma (<0.3) Re=1~3000	Br (<0.005)	λ (<0.01) Re=1~3000	*Pe* (>50) Re=1~3000
D_h=180 μm	gas	0.00007	0.0006~0.10	1.5×10^{-6}	2.18~0.005	10~2340
	liquid	0.00001	0.0003~0.04		0.10~0.0002	3~200
D_h=110 μm	gas	0.00012	0.0018~0.27	2.9×10^{-6}	1.63~0.006	10~2400
	liquid	0.00002	0.0007~0.11		0.80~0.0002	5~200
D_h=65 μm	gas	0.00021	0.0031~0.46	8.7×10^{-6}	1.10~0.002	8~2430
	liquid	0.00005	0.0010~0.20		0.20~0.0004	5~2700

heating relative to the conductive heat transfer. The viscous effect can be considered negligible if the *Br*<0.005 during the test. Axial conduction effects in the wall can be monitored by the conduction parameter, $\lambda = k_w A_c/(\dot{m} c_P L_h)$. Usually the axial conduction effect in the wall can be considered negligible if the conduction parameter is less than 0.01. Axial conduction of the fluid can be monitored by the Peclet number (Pe=Re · Pr), and it can be neglected for Pe >50.

Table 3 shows the typical range of non-dimensional numbers for the Reynolds number range from 1 to 3000. From these data it can be concluded that rarefaction effects, compressibility effects, and viscous effects are negligible. The axial conduction effects through the wall and fluid become considerable when the Reynolds numbers are small. However, the axial conduction effects through the wall have more impact than the axial conduction through the fluid, when comparing the orders of magnitude of λ and Pe. For example, when Re=1 for D_h=65μm tube, the λ is 1.10 compared to the 0.01, and the Pe is 8 compared to 50. Therefore, it is assumed that the axial conduction effects in the solid influenced the measurement.

Maranzana *et al*[14] analytically solved the temperature profile of the wall and fluid, and concluded that the fluid temperature profile becomes non-linear in the axial direction. They also mentioned that the heat flux to the fluid is not uniform over the heating length when axial conduction through the wall is present. During the data reduction process in the experiment, it is customary to assume the heat flux is uniform over the length, and temperature increases in linear profile. They concluded that the fluid temperature difference between the non-linear and the linear profile makes the Nusselt number dependent on the Reynolds number.

Lin and Kandlikar[18] derived an equation to estimate the degradation of Nusselt number due to the axial conduction effects as eqn. (7). The heat transfer coefficient when the axial conduction dominant condition and that of regular condition is compared by the 1st law of thermodynamics. The comparison result can be summarized as eqn. (7), where the details are fully explained in the literature [18]

$$\frac{Nu_{app}}{Nu_{theory}} = \frac{h_{app}}{h_x} = \frac{1}{1+4\dfrac{k_w}{k_f}\dfrac{A_w}{A_f}\dfrac{Nu_{theory}}{(\mathrm{Re}\,\mathrm{Pr})^2}} \tag{7}$$

The degradation amount for the estimated Nusselt number is related to the property and the flow rate of the fluid, the thermal conductivity ratio between wall (k_w) and fluid (k_f), and cross sectional area ratio between wall (A_w) and fluid (A_f). The flow condition (Reynolds number (Re), Prandtl number (Pr)) is also related to the reduction of Nusselt number. They indicated that apparently the Nusselt number shows degraded value (Nu_{app}) in the experiments compared to the theoretical value (Nu_{theory}) due to the axial conduction effects. Eqn (7) also indicates that the heat transfer coefficient for laminar flow holds constant. The axial conduction effect in the wall affects not only the wall temperature profile, but also the fluid temperature profile in the channel. Thereby, the axial conduction effect influences the

assumption of the measurement, thereby rendering the estimated Nusselt number to become an value.

Figure 5 also displays the apparent Nusselt number calculated from eqn (7) for various operating conditions for three different microchannels. For the calculation results for the nitrogen gas, Nu_{app} decreases rapidly when Reynolds numbers are less than 1000. The Nu_{app} for the D_h=180 μm channel show highest value, and the Nu_{app} for the D_h=110 μm channel show the lowest values. The calculated Nu_{app} for three different microchannels show very similar trend with the experimental results. The relative magnitude of Nu_{app} for the microchannels follows sequence with the experimental results. The calculated Nu_{app} for the liquid nitrogen show deviations from the experimental results. However, the value of Nu_{app} are much greater than those for gas nitrogen. Such different values of Nu_{app} are derived from the thermo-physical property change of the fluid and the microchannel.

From the comparison, it can be concluded that the measurements are affected by the axial conduction effects, and estimated Nusselt number from the experimental values are the apparent Nusselt number. Moreover, the comparison validates the theoretical Nusselt number in the microchannel also holds constant in laminar flow regime.

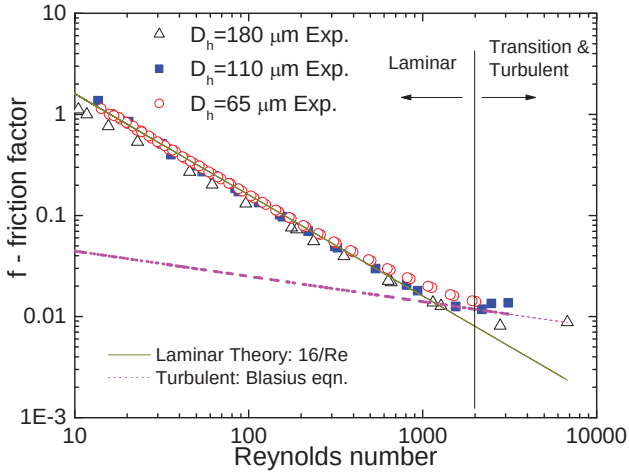

Figure 4 Friction factor comparison between the measurement and theory (part of data shown for clarity)

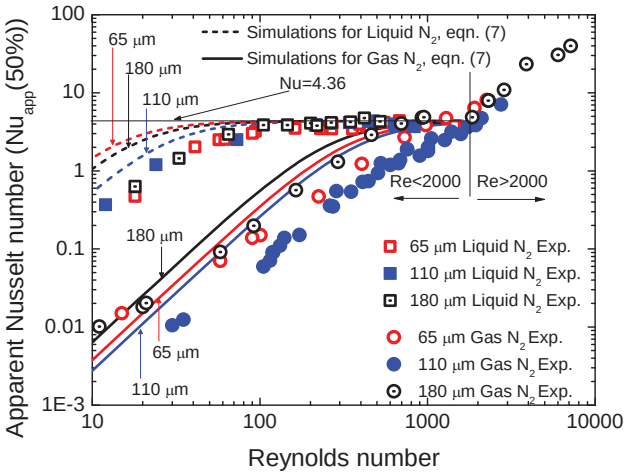

Figure 5 The comparison of the apparent Nusselt number $Nu_{app}(50\%)$ between the experimental results (eqns (2)~(6)) and calculated value from eqn. (7).

4. Conclusion

The hydraulic and thermal characteristics of fluid in the microchannel are investigated by the experiments. The measured friction factors are comparable to those in macro-scale tubes. The experimental results of the heat transfer indicate that Nusselt numbers derived from measurements are significantly affected by axial conduction at low Reynolds flow. The axial conduction effects change the fluid temperature profile to become non-linear. The measured Nusselt numbers, based on the classical assumption of a linear temperature profile begin to deviate from the true value and are referred to as apparent Nusselt numbers. The comparison between the experimental results and theoretically derived apparent Nusselt number implies that the Nusselt numbers hold constant in the laminar flow regime for single-phase fluid.

5. Acknowledgement

We gratefully acknowledge DARPA FPA-MCC program for funding support.

6. Reference

[1] Radebaugh R, 2014 *AIP Conference Proceedings* **1573** (1) 132-141
[2] Morini G L, 2004 *International Journal of Thermal Sciences* **43** 631-651
[3] Asadi M, Xie G and Sunden B, 2014 *International Journal of Heat and Mass Transfer* **79** 34-53
[4] Lin M H, Bradley P E, Huber M L, Lewis R, Radebaugh R and Lee Y C, 2010 *Cryogenics* **50** (8) 439-442
[5] Lewis R, Wang Y, Schneider H, Lee Y C and Radebaugh R, 2013 *Cryogenics* **57** 140-149
[6] Lewis R, Wang Y, Bradley P E, Huber M L, Radebaugh R and Lee Y C, 2013 *Cryogenics* **54** (0) 37-43
[7] Radebaugh R, Bradley P, Coolidge C, Lewis R and Lee Y C, 2014 *The 18th International Cryocooler Conference* **18** 377-388
[8] Peng X F and Peterson G P, 1996 *International Journal of Heat and Mass Transfer* **39** (12) 2599-2608
[9] Wu P and Little W A, 1984 *Cryogenics* **24** 415-420
[10] Choi S, Barron R and Warrington R, 1991 *ASME DSC* **32** 123-134
[11] Moffat R J, 1988 *Experimental Thermal and Fluid Science* **1** (1) 3-17
[12] Yang C-Y, Chen C-W, Lin T-Y and Kandlikar S G, 2012 *Experimental Thermal and Fluid Science* **37** (0) 12-18
[13] Morini G L, Yang Y and Lorenzini M, 2012 *Experimental Heat Transfer* **25** (3) 151-171
[14] Maranzana G, Perry I and Maillet D, 2004 *International Journal of Heat and Mass Transfer* **47** (17-18) 3993-4004
[15] Lemmon E W, Huber M L and McLinden M O, (National Institute of Standards and Technology, Standard Reference Data Program, Gaithersburg, 2010).
[16] Incopera F and De Witt D, (Prentice-Hall, New York, 1990).
[17] Guo Z-Y and Li Z-X, 2003 *International Journal of Heat and Mass Transfer* **46** (1) 149-159
[18] Lin T-Y and Kandlikar S G, 2012 *Journal of Heat Transfer* **134** (2) 020902